EasyChair Preprint

№ 9332

Analysis of Kuramoto Models for AC Microgrids Based on Droop Control

Qing Xu, Shitao Wang, Jiayi Liu, Huihui Song and Yanbin Qu

November 17, 2022

Analysis of Kuramoto models for AC microgrids based on droop control

1st Qing Xu
College of New Energy
Harbin Institute of Technology (Weihai)
Weihai, China
1283740254@qq.com

2nd Shitao Wang
Educational Administration Center
State Grid of China Technology College
Jinan, China
wangst_chn@hotmail.com

3rd Jiayi Liu
College of New Energy
Harbin Institute of Technology (Weihai)
Weihai, China
19b906023@stu.hit.edu.cn

4th Huihui Song
College of New Energy
Harbin Institute of Technology (Weihai)
Weihai, China
songhh@hitwh.edu.cn

5th Yanbin Qu
College of New Energy
Harbin Institute of Technology (Weihai)
Weihai, China
quyanbin@hit.edu.cn

***Abstract*—As a typical nonlinear coupled system, microgrid has nonlinear coupling relationships between generations and distributions which cannot be ignored. In this paper, the problem of power balance between distributed generators and loads is transformed into the motion synchronization problem of multiple Kuramoto coupled oscillators. And this paper proposes to model an islanded microgrid by using a second-order Kuramoto model. By exploiting the model, our key sight is to address the transient stability problem and find a trapping region expressed explicitly in the parameters. Finally, the similarity between transient stability of islanded microgrid and frequency synchronization of Kuramoto coupled oscillators is analyzed, and the validity of microgrid Kuramoto models is verified based on the 3-generator 5-node islanded microgrid MATLAB/ Simulink simulation platform.**

***Index Terms*—Microgrid; Kuramoto model; droop control; transient stability; the trapping region.**

I. Introduction

As one of the leading technologies, microgirds have been envisioned to increase the penetration of the new generation facilities in power market [1]. And power electronics plays an essential role that allows inverters in the microgrids to emulate desired dynamic behaviors of conventional power system. In the process of emulating, synchronization of microgrid is an important issue in relation to the transient stability [2].

Recent years, scholars have discovered that the units of power network systems are closely related to the interacted Kuramoto coupled oscillators, in particular, the similarity between frequency synchronization of Kuramoto oscillators and transient stability of power network [3]. [4] derived the second-order Kuramoto model of conventional power system through the principle of conservation between generators power production and motors power consumption. [5]–[7] have successfully applied the first-order Kuramoto model synchronization theory to the transient stability analysis of power system. And based on this model, the first-order Kuramoto model and the structure-reserved power system model have been proved to have the same local synchronization property and local stability property. Moreover, synchronization in the first and second-order Kuramoto models and a smart grid application with loads and generators were considered by [8]. But the authors mainly focused on the grid topology and mentioned that, "Another important question not addressed in the present article concerns the region of attraction of a synchronized solution." It is pointed out in survey paper [9] that the transient dynamics of second-order oscillator network is a challenging open problem.

In view of the diversity of microgrid distributed energy resource (DER) units and regulation characteristics, and the particularity of islanded mode, microgrids Kuramoto models are proposed in this paper. Then, we investigate the inertial characteristics of the units in the microgrid. Considering the low-frequency mode of droop controller, a second-order Kuramoto model for inveters in microgird are proposed. Based on the second-order Kuramoto model, we find a trapping region such that the phase of the microgrid units located in this region will evolve into a synchronous state. Finally, we discuss the critical condition that the power perturbations do not destroy the transient stability, whether the phase of microgrid units is still located in the trapping region under perturbations. And we give a theoretical framework which consideres generator application by numerical simulations in [4] .

The outline of the rest paper is as follows. In Section II, we propose a second-order Kuramoto model of microgrid. In Section III, we give some general theorems for the transient stability analysis of microgrid system. The simulations are given in Section IV, and the theoretical results are verified experimentally on a prototype microgrid. The paper is concluded in Section V.

This work was supported in part by the NNSF of China under Grant (No. 61773137), in part by the NNSF of Shandong Province (No. ZR2019MF030), in part by China Postdoctoral Science Foundation (No. 2018M641830).

II. Modeling for a microgrid by Kuramoto Model

A. The multirate Kuramoto model of microgrid

Consulting the second-order Kuramoto model of conventional multi-generators power system and considering the difference between the conventional power system and the microgrid, the multirate Kuramoto model is utilized to cast the universal microgrid. In conclusions of reference [4], [8], [10], the universal microgrid can be described as,

$$\begin{cases} M_i\ddot{\theta}_i + D_i\dot{\theta}_i = P_{N,i} + \underbrace{p_i}_{\text{regulation}} \\ \qquad\qquad \underbrace{-\sum_{j=1}^{n} a_{ij}\sin(\theta_i - \theta_j)}_{P_{e,i}}, i \in V_1 \\ D_i\dot{\theta}_i = P_{N,i} + \underbrace{p_i}_{\text{regulation}} \\ \qquad\qquad \underbrace{-\sum_{j=1}^{n} a_{ij}\sin(\theta_i - \theta_j)}_{P_{e,i}}, i \in V_2 \end{cases} \tag{1}$$

where V_1 and V_2 are the sets of DER units with inertial and without inertia, respectively. θ_i and $\dot{\theta}_i$ denote phase (rad) and frequency deviation (Hz) of the i-th unit. θ_j is the phase (rad) of the j-th unit coupled with the i-th unit. φ_{ij} is the initial phase deviation between the units i and j (rad). If the left side of equation (1) is zero, then the DER units can be seen as constant power output. Moreover, the rated power (p.u.) of the i-th unit is described by $P_{N,i}$, and the regulation of the DER units output power is represented by p_i. Thus, the power reference value of the i-th unit is $P_{N,i} - p_i$:

A. $P_{N,i} > 0 \rightarrow$ generator units, $P_{N,i} < 0 \rightarrow$ load unit, P_N, i can be positive or negative $\rightarrow$ energy storage unit.

B. $p_i \neq 0 \rightarrow$ the rated power is adjustable. $p_i = 0 \rightarrow$ the rated power cannot be adjusted.

The different combinations of A and B can contain most of the units in microgrids with different regulation characteristics. Seen from the multirate Kuramoto model of Equ. (1) , the first formula of Equ. (1) is the second-order Kuramoto coupled-oscillator model structure, describing the inertial units. And the second formula of Equ. (1) is the first-order Kuramoto coupled-oscillator model, describing the inertialess units.

B. Kuramoto Models of Inertialess units and Inverter units

The differences in the physical structure of each DER unit result in different sensitivities to apperceive the changes of microgrid system frequency. Such as variable speed wind turbine and flywheel energy storage, etc. should be classified as inertialess generator units. However, the inertialess DER units with inverters as the interface have some good controlled characteristics. The droop controller is proposed to emulates the behavior of a classical synchronous generator [11]]. The second formula of Equ. (1) casts the inverter unit with droop control of microgrid. Moreover, the microgrids include several special inertialess units. In islanded or grid-connected mode, the Kuramoto model of switch at Point of Common Coupling (PCC) is showed in Equ. (2) and (3). And the model of constant power type loads is showed in Equ. (4). The model of Constant admittance type loads usually follows from Kron reduction.

$$0 = P_{N,i} - \sum_{i=1}^{N} E_i E_j \mid Y_{ij} \mid \sin(\theta_i - \theta_j + \varphi_{ij}) \tag{2}$$

$$0 = \sum_{j=1}^{N} E_i E_j \mid Y_{ij} \mid \sin(\theta_i - \theta_j + \varphi_{ij}) \tag{3}$$

$$0 = -P_{N,i} - \sum_{j=1}^{N} E_i E_j \mid Y_{ij} \mid \sin(\theta_i - \theta_j + \varphi_{ij}) \tag{4}$$

Through the investigation of inertial characteristics, in the consideration of some inertial elements, it is found that the droop controller of inverter can also be established as a second-order Kuramoto model like a synchronous generator rotor. This will facilitate the coordinated control and unified analysis of synchronous generators and inverter units in microgrid systems. With the analysis of the microgrid units inertial characteristics, it can be seen that the weak coupling between the inverter units and the microgrid results in the unresponsiveness of the units to the frequency changes of the system.

However, the conventional frequency droop control (CFDC) uses the inverter active power output frequency to simulate the inertial behavior of synchronous generator in power system, which ensures the power sharing between inverters and the frequency stability of the system. The authors [11] use the first-order Kuramoto model to cast linear frequency droop control law of parallel inverters. The enlightening method relaxes some assumptions of the conventional droop control, which is greatly effective to study the synchronization of inverters.

Nevertheless, this model only takes the droop law of the droop controller into account. To ensure the time scale division, low frequency mode of the outer power control loop with a bandwidth of 2-10Hz is usually designed to improve stability and power quality injected to the droop controller. Considering the inertial behavior generated by the low-frequency mode, the relationship between ω_i and p_i is no longer strictly linear. Moreover, when operating at a nominal frequency, to obtain a wider range of regulation, linear law usually sets $P^* = 0$. However, for relaxing the assumption of droop coefficients, it may be better to set $P^* = P_{N,i} \in (0, \bar{P}_i)$. Motivated by above two factors, considering the influence of the low-pass filter, this paper proposes a second-order Kuramoto model to characterize the inverter unit with droop controller. The control formula is as follows

$$\Delta\omega = m_i(P_{N,i} - \frac{\omega_c}{\omega_c + s}p_i), \tag{5}$$

where ω_c is cutoff frequency of low-pass filter which produces the low-frequency mode. τ is the time constant, $\tau = 1/\omega_c$. Equ. (5) can be reformed as

$$\begin{aligned} \omega_i &= \omega^* + m_i P_{N,i} - \frac{m_i}{\tau s + 1} p_i \\ m_i &= \frac{\omega_* - \omega_{\min}}{P_{i\max} - P_{N,i}}, \end{aligned} \tag{6}$$

where ω^* is the nominal frequency of the microgrid. $P_{N,i}$ represents the active rated capacity. m_i is the gain of active power droop control. p_i describes the instantaneous active power of inverter when running at the frequency ω_i. The distributed generation i (DGi) output maximum active power is denoted by $P_{i\max}$. $\omega_{\min}$ is the system minimum frequency. Equ. (6) can be simplified as following

$$\tau m_i^{-1} \frac{d\left(\omega_i - \omega^*\right)}{dt} + m_i^{-1}\left(\omega_i - \omega^*\right) = P_{N,i} - p_i. \tag{7}$$

Making $\dot{\theta}_i = \omega_i - \omega^*$, $M_i = \tau m_i^{-1} = m_i^{-1}\omega_c^{-1}$, $D_i = m_i^{-1}$, and substituting into Equ. (7), then we derived that

$$M_i \ddot{\theta}_i + D_i \dot{\theta}_i = P_{N,i} - p_i. \tag{8}$$

Considering the *n* nodes microgrid composed of DER units and loads, the inductance line between nodes i and j is expressed by admittance $|Y_{ij}|$. The injected instantaneous active power of node i is

$$p_i = \sum\nolimits_{j=1}^{l} E_i E_j |Y_{ij}| \sin\left(\theta_i - \theta_j\right) - \Delta\hat{p}_i. \tag{9}$$

Therefore, the inverter units with the droop controller can be reformed as

$$M_i \ddot{\theta}_i + D_i \dot{\theta}_i = P_{N,i} + \sum\nolimits_{j=1}^{l} E_i E_j \left|Y_{ij}\right| \sin\left(\theta_j - \theta_i\right) + \Delta\hat{p}_i, \tag{10}$$

where E_i and E_j are voltage amplitude values for inverter units i and j.

III. Transient stability analysis of microgird

According to 2.2, we obtain a uniform second-order Kuramoto model of microgrid. With different damping coefficient D_i and inertia coefficient M_i ($D_i M_i^{-1}$ is constant), this model can include almost the frequency control units in the AC microgrids. When the microgrid emulates the operation of the conventional power system, this will be beneficial to the coordinated control and unified analysis of units in the microgrid. On the basis of the proposed secondary-order Kuramoto model of microgrid and some mathematical theories, a key estimate of the trapping region has been given. We ignore $\Delta\tilde{p}_i$ influence in this subsection. Thus, the second-order Kuramoto model of microgrid can be represented by

$$M_i \ddot{\theta}_i + D_i \dot{\theta}_i = P_{N,i} + \sum_{j=1}^{n} a_{ij} \sin\left(\theta_j - \theta_i\right), \tag{11}$$

$$\sum_{i=1}^{n} P_{N,i} = 0, \gamma = D_i M_i^{-1}, \quad i = 1, 2, ...n. \tag{12}$$

For an ensemble of phase $\theta\left(t\right) = \left(\theta_1\left(t\right), \theta_2\left(t\right), ..., \theta_n\left(t\right)\right)$, setting is as follows,

$$\theta_m = \min_{1\le i\le n} \theta_i, \quad \theta_M = \max_{1\le i\le n} \theta_i,$$

$$\theta_\theta = \theta_M - \theta_m, \quad \dot{\theta}_\theta\left(0\right) = \frac{\mathrm{d}\theta_\theta\left(t\right)}{\mathrm{dt}}|_{t=0+}, \tag{13}$$

$$C\left(\theta_0, \dot{\theta}_0, \alpha\right) = \max\left\{\theta_\theta(0), \theta_\theta(0) + \gamma^{-1}\dot{\theta}_\theta(0)\right\}, \tag{14}$$

$$p\left(P_{N,i}\right) = \max_{1\le i\le n}\left\{M_i^{-1} P_{N,i}\right\} - \min_{1\le i\le n}\left\{M_i^{-1} P_{N,i}\right\}, \tag{15}$$

$$A = \min_{1\le i\ne j\le n}\left\{\left(M_i^{-1} + M_j^{-1}\right) a_{ij} + \sum_{k\ne i,j} \min\left\{M_i^{-1} a_{ik}, M_j^{-1} a_{ik}\right\}\right\} \tag{16}$$

Thanks to (11) , we have

$$\ddot{\theta} + \gamma\dot{\theta}_i = M_i^{-1} P_{N,i} + M_i^{-1} \sum_{j=1}^{N} a_{ij} \sin\left(\theta_j - \theta_i\right). \tag{17}$$

Here, the following relation has been utilized

$$\begin{aligned} & \sin\left(\theta_j - \theta_M\right) - \sin\left(\theta_j - \theta_m\right) \\ = \;& 2\cos\left(\frac{2\theta_j - \theta_M - \theta_m}{2}\right)\sin\left(-\frac{\theta_\theta\left(t\right)}{2}\right) \\ \le \;& -2\cos\left(\frac{\theta_\theta\left(t\right)}{2}\right)\sin\left(\frac{\theta_\theta\left(t\right)}{2}\right) \\ = \;& -\sin\theta_\theta\left(t\right). \end{aligned} \tag{18}$$

If $A > 0$, $\theta_\theta\left(t\right) \in \left(0, \pi\right)$, then

$$\begin{aligned} & \ddot{\theta}_\theta\left(t\right) + \gamma\dot{\theta}_\theta\left(t\right) \\ = \;& M_M^{-1} P_{N,M} - M_m^{-1} P_{N,m} + M_M^{-1} \sum_{j=1}^{n} a_{Mj} \sin\left(\theta_j - \theta_M\right) \\ - \;& M_m^{-1} \sum_{j=1}^{n} a_{mj} \sin\left(\theta_j - \theta_m\right) \\ \le \;& p\left(P_{N,i}\right) + M_M^{-1} \sum_{j=1}^{n} a_{Mj} \sin\left(\theta_j - \theta_M\right) \\ - \;& M_m^{-1} \sum_{j=1}^{n} a_{mj} \sin\left(\theta_j - \theta_m\right) + M_M^{-1} a_{Mm} \sin(\theta_m - \theta_M) \\ - \;& M_m^{-1} a_{mM} \sin(\theta_M - \theta_m) \\ \le \;& p\left(P_{N,i}\right) - A\sin\theta_\theta\left(t\right). \end{aligned} \tag{19}$$

Moreover, let $A \ge p\left(P_{N,i}\right)$ and $\bar{\theta} \in \left(0, \frac{\pi}{2}\right)$ is determined by the equation $\sin\bar{\theta} = p(P_{N,i})A^{-1}$. If $\theta_\theta \in \left(\bar{\theta}, \pi - \bar{\theta}\right)$, and the initial condition satisfies $0 \le C\left(\theta_0, \dot{\theta}_0, \gamma\right) < \pi - \bar{\theta}$, without loss of generality, we note that by (19)

$$\ddot{\theta}_\theta\left(t\right) + \gamma\dot{\theta}_\theta\left(t\right) \le p\left(P_{N,i}\right) - A\sin\theta_\theta\left(t\right) < 0. \tag{20}$$

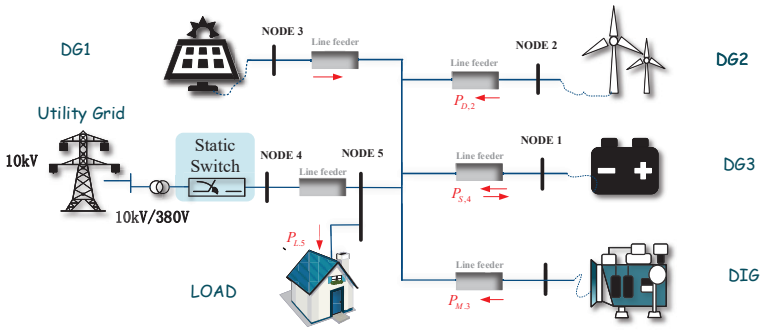

Fig. 1. The network topology of microgrid system. square figure of system (4) when $l = 4$.

If $\theta_\theta(t)$ never drops to $\bar{\theta}$, it is easy to derive that for all $t > 0$

$$\theta_\theta(t) \leq \theta_\theta(0) + \gamma^{-1}\left(1 - e^{-\gamma t}\right)\dot{\theta}_\theta(0) \leq C\left(\theta_\theta, \dot{\theta}_\theta, \gamma\right). \tag{21}$$

IV. Simulation Study

In this paper, three kinds of inverter-based distributed generators (DG1, DG2 and DG3), a small diesel electric generator (DIG) and a constant power type load (Load) are configured in the simulation model of microgrid. This paper focuses on the dynamic characteristics of microgrid system whose configuration occupied by power electronic devices. Therefore, to clearly characterize the impact of inverter-based distributed generators, the DIG (synchronous generator) in the simulation process is set up to output constant 200 kW active power value. And the line impedance parameters and node parameters are given in TABLE I and Table II , respectively. The network topology of the microgrid system is shown in Fig.1.

TABLE I: Parameters of each node

No.	*Unit Name*	$M_i(\times 10^4)$	$D_i(\times 10^4)$	$P_{M,i}(\times 10^4)$	E_i
1	DG1	0.17	1.67	3	310
2	DG2	0.83	0.83	1	310
3	DG3	0.56	0.56	2	310
5	DIG+LOAD	0.33	3.33	-6	310

TABLE II: Parameters between nodes ($\varphi_{ij} = \arctan(G_{ij}/B_{ij})$)

No.	$R + jX$	$a_{ij}(\times 10^4)$	φ_{ij}
1-2	1.2820+j5.36$\times 10^{-3}$	3.77	0
1-3	1.2820+j5.36$\times 10^{-3}$	3.77	0
1-5	0.0641+j2.68$\times 10^{-3}$	7.54	0
2-3	1.2820+j5.36$\times 10^{-3}$	3.77	0
2-5	0.0641+j2.68$\times 10^{-3}$	7.54	0
3-5	0.0641+j2.68$\times 10^{-3}$	7.54	0

Based on the above analysis, this case investigates the similarity between the frequency synchronization of the Kuramoto coupled oscillators and the transient stability of microgrid in normal operation, perturbation process or failure process. The simulation results are shown in Fig.2, Fig.3 and Fig.4. Fig.3 shows the simulation results of Kuramoto coupled oscillators

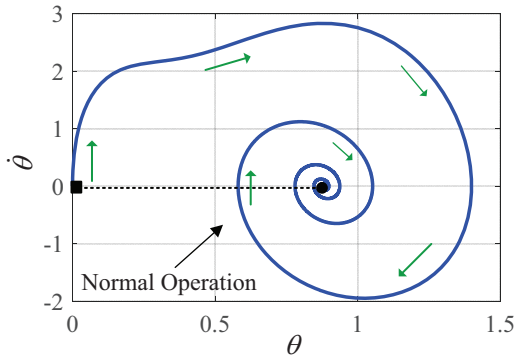

(a) Frequency simulation comparison between each DG unit in Kuramoto coupled oscillator model.

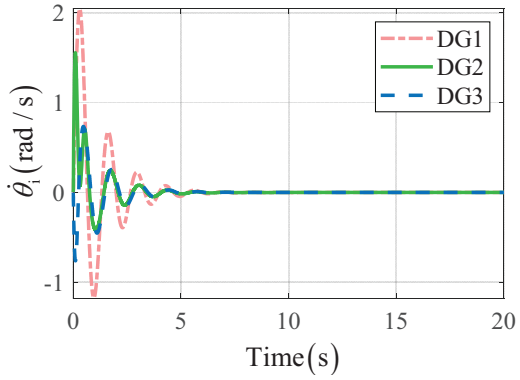

(b) Frequency simulation comparison between each DG unit in Kuramoto coupled oscillator model.

Fig. 2. Frequency simulation diagram under the effect of constant power-type load in normal operation.

dynamic characteristics and microgrid transient characteristics in perturbation process. Fig.4 shows the simulation results of failure process about Kuramoto coupled oscillators frequency synchronization and microgrid transient stability.

Comparing Fig.2, Fig.3 and Fig.4, the simulation results further validate the effectiveness of modeling a microgrid system by the second-order Kuramoto model. And the similarity between the frequencies of Kuramoto coupled oscillators and the transient stability of microgrid is further validated. Moreover, Fig.2, Fig.3 and Fig.4 test and verify the magnitude and the removal time of the perturbation are the key to determining whether the microgrid can be stabilized.

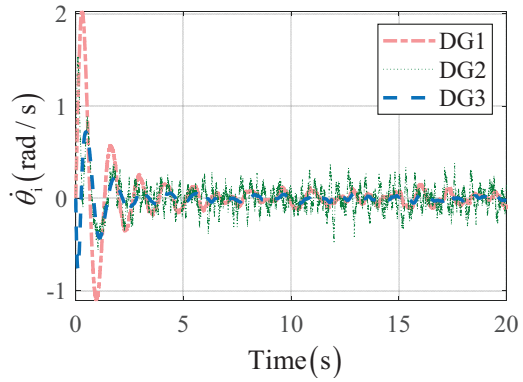

(a) Frequency simulation comparison between each DG unit in Kuramoto coupled oscillator model.

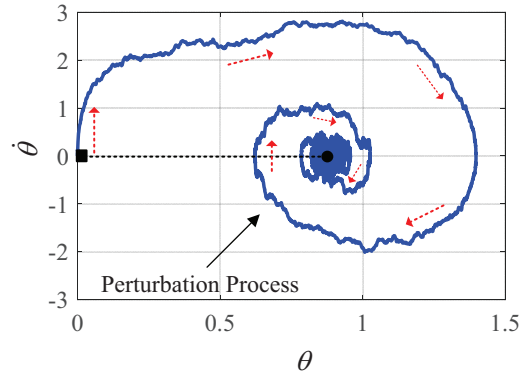

(b) Frequency simulation comparison between each DG unit in Kuramoto coupled oscillator model.

Fig. 3. Frequency simulation diagram under the effect of constant power-type load in perturbation process.

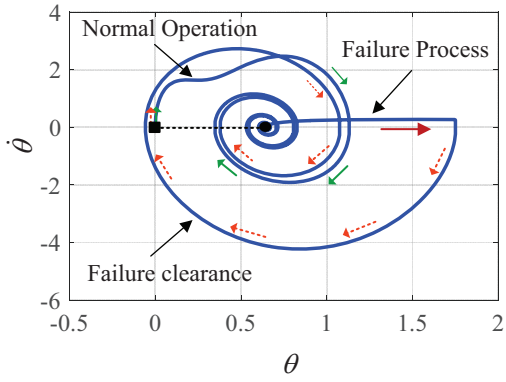

(a) Frequency simulation comparison between each DG unit in Kuramoto coupled oscillator model.

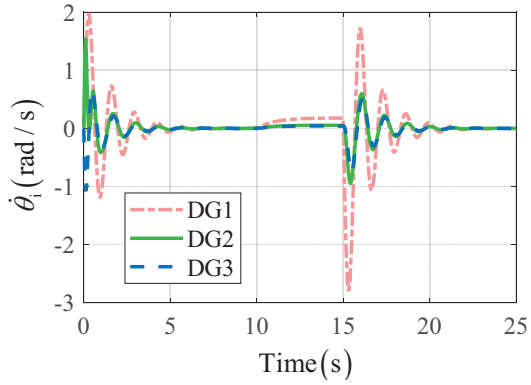

(b) Frequency simulation comparison between each DG unit in Kuramoto coupled oscillator model.

Fig. 4. Frequency simulation diagram under the effect of constant power-type load in failure process.

V. Conclusion

By analyzing the transient characteristics of the microgrid system and the dynamic characteristics of the coupled oscillator network, it is noticed the similarity between the oscillator synchronization problem of dynamic network and the transient stability problem of microgrid. The transient characteristics of the interacting network nodes in the microgrid can be described by the synchronization theory of the Kuramoto coupled oscillator in the dynamic network. It helps more from the perspective of dynamics throughout understanding of the transient characteristics of islanded microgrid operation. And it is the key dealing with the transient stability problem of microgrid, such as finding the trapping region of microgrid system in this paper. Furthermore, based on the estimate of the trapping region, the relationship between the perturbation and its duration has been derived under critical stability. It is verified that the effectiveness of modeling the microgrid by a second-order Kuramoto model as well as the similarity between the transient stability of islanded microgrid and the frequency synchronization of Kuramoto oscillator.

References

[1] C. De Persis and N. Monshizadeh, "Bregman storage functions for microgrid control," *IEEE Transactions on Automatic Control*, vol. 63, no. 1, pp. 53–68, 2017.

[2] J. W. Simpson-Porco, F. Dörfler, and F. Bullo, "Synchronization and power sharing for droop-controlled inverters in islanded microgrids," *Automatica*, vol. 49, no. 9, pp. 2603–2611, 2013.

[3] L. Zhu and D. J. Hill, "Stability analysis of power systems: A network synchronization perspective," *SIAM Journal on Control and Optimization*, vol. 56, no. 3, pp. 1640–1664, 2018.

[4] G. Filatrella, A. H. Nielsen, and N. F. Pedersen, "Analysis of a power grid using a kuramoto-like model," *The European Physical Journal B*, vol. 61, no. 4, pp. 485–491, 2008.

[5] F. Dörfler and F. Bullo, "On the critical coupling for kuramoto oscillators," *SIAM Journal on Applied Dynamical Systems*, vol. 10, no. 3, pp. 1070–1099, 2011.

[6] F. Dörfler and F. Bullo, "Kron reduction of graphs with applications to electrical networks," *IEEE Transactions on Circuits and Systems I: Regular Papers*, vol. 60, no. 1, pp. 150–163, 2012.

[7] F. Dörfler and F. Bullo, "Synchronization of power networks: Network reduction and effective resistance," *IFAC Proceedings Volumes*, vol. 43, no. 19, pp. 197–202, 2010.

[8] F. Dörfler, M. Chertkov, and F. Bullo, "Synchronization in complex oscillator networks and smart grids," *Proceedings of the National Academy of Sciences*, vol. 110, no. 6, pp. 2005–2010, 2013.

[9] F. Dörfler and F. Bullo, "Synchronization in complex networks of phase oscillators: A survey," *Automatica*, vol. 50, no. 6, pp. 1539–1564, 2014.

[10] F. Dörfler and F. Bullo, "Topological equivalence of a structure-preserving power network model and a non-uniform kuramoto model of coupled oscillators," in *2011 50th IEEE Conference on Decision and Control and European Control Conference*. IEEE, 2011, pp. 7099–7104.

[11] J. W. Simpson-Porco, Q. Shafiee, F. Dörfler, J. C. Vasquez, J. M. Guerrero, and F. Bullo, "Secondary frequency and voltage control of islanded microgrids via distributed averaging," *IEEE Transactions on Industrial Electronics*, vol. 62, no. 11, pp. 7025–7038, 2015.